Analysis of first and second order surface processes in fusion solid breeders

Alya A. Badawi

Nuclear Engineering Department, Alexandria University Alexandria, Egypt

Surface reactions in tritium release from fusion ceramic breeders were investigated. Analyses of the tritium inventory were made under steady state conditions using first and second order adsorption/desorption processes on the surface. The resulting equations were used to calculate the grain and surface inventories for different temperatures ranging from 350°C to 900°C, and different H_2 concentrations ranging from 0% to 10%, using data from Li_2O samples resulted from the experiments named TTTEx. Comparison between the analysis and the experimental data leads to the conclusion that in order to study the behavior of tritium inside the ceramic breeders, second order surface processes must be used in modeling and calculating the tritium release and inventory. Although this analysis used data from Li_2O samples, there would be no need to repeat the calculations using other materials. The results of this study apply to most ceramic breeders, since the tritium exhibits the same behavior when other materials are used.

تمت في هذا البحث دراسة تفاعلات السطح لتحرير التريتيوم من مولدات الاندماج الخزفية. كما تم تحليل جرد التريتيوم في الحالات الثابتة مع الزمن , و ذلك باستخدام عمليات أدمصاص و مج من الدرجة الأولى و الثانية على السطح. استعملت المعادلات الناتجة لحساب الجرد في الحبيبات و على السطح لدرجات حرارة مختلفة بين ٣٥٠ و ٩٠٠ درجة مئوية, و تركيز هيدروجين مختلف بين ٠% و ١٠% , باستخدام البيانات الخاصة بعينات أكسيد الليثيوم المستخدمة في مجموعة تجارب TTTEx. أدت المقارنة بين التحليل النظري و النتائج التجريبية إلى أنه حتى يمكن دراسة سلوك التريتيوم داخل المولدات الخزفية, يجب استخدام عمليات سطح من الدرجة الثانية في النماذج الموضوعة لحساب تحرير و جرد التريتيوم.
بالرغم من استخدام البيانات الخاصة بعينات أكسيد الليثيوم, فانه من الممكن تطبيق نفس النتيجة على أغلبية المولدات الخزفية, و ذلك لأن سلوك التريتيوم متشابه في معظم المولدات الخزفية.

Keywords: Solid breeders, Adsorption, Desorption, Surface coverage, Tritium inventory.

1. Introduction

Precise evaluation of tritium inventory in the fusion blanket is essential for the design of the fusion reactor fuel cycle. Tritium transport and release from the solid breeding material are complex processes that include both diffusion as well as surface reactions (such as adsorption, desorption, and dissolution processes)[1]. The rate-limiting process is dependent on the operating conditions, such as temperature, purge gas composition, and microstructure parameters such as grain size and porosity distribution [2]

It has been reported that at high temperature the rate-determining processes of tritium release are surface process [3]. Also, at high temperatures, the surface inventory was found to be larger than that due to diffusion in the absence of H_2 or water vapor in the purge gas [4].

In most studies, adsorption/desorption processes are considered to be first-order reactions. However, in some experiments it was found that they can be of a second order [5]. Hence, there is a need to know how the modeling results will differ in each case, as well as find out whether both first and second order reactions can be used to simulate the phenomena associated with tritium transport in ceramic breeders.

In this paper, the effect of the order of surface reactions was investigated. Both the tritium inventories in the grain and on the surface were examined as a function of temperature, in the presence and absence of H-atoms in the purge gas. Data from the TTTEx experiments [6-10] were used to calculate the surface and grain inventories in different conditions. The phenomena studied in this paper are the decrease of tritium inventory with increasing temperature, and its

decrease with the addition of H_2 to the sweep gas. Steady state was assumed to simplify the equations to be solved analytically and not numerically as in the case of transient conditions. This gives a better understanding of the phenomena involved in the tritium release and retention. It should be noted that using either steady state or transient conditions has no effect on the order of surface reactions, which is the focus of this paper.

2. The surface fluxes

A schematic diagram showing the fluxes due to different processes on the surface is shown in Figure 1. There are mainly 4 fluxes going to and from the surface [11]:

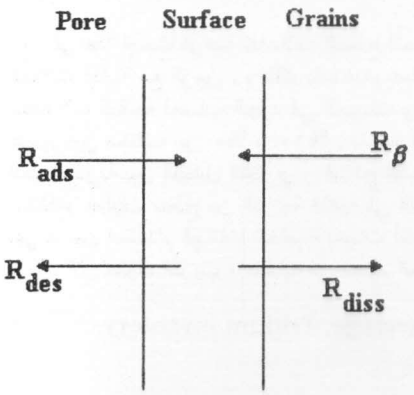

Fig. 1. Schematic diagram showing the different surface fluxes.

1. A flux, R_{ads} (at/m².s), going from the pore to the surface. For first order adsorption [11],

$$R_{ads} = \frac{\sigma.z}{\sqrt{8\times10^{-3}\pi}}\sqrt{\frac{RT}{M}}C_p(1-\theta)\exp(-E_{ads}/RT). \quad (1)$$

Where C_p is the concentration of the adsorbed species in the pore (at/m³), θ is the total surface coverage (i.e. the fraction of filled surface sites). The term (1 - θ) represents the number of empty sites available for adsorption. E_{ads} is the activation energy of adsorption (J/mol), R is the universal gas constant (J/mol.K), T is the temperature (K), σ is the sticking coefficient, z is the number of sites adjacent to each atom, and M is the molecular weight. For second order adsorption [12],

$$R_{ads} = \frac{\sigma.z}{\sqrt{8\times10^{-3}\pi}}\sqrt{\frac{RT}{M}}C_p(1-\theta)^2\exp(-2E_{ads}/RT). \quad (2)$$

Note that the squaring of (1 - θ) and the doubling of E_{ads} stems from the fact that two atoms are required to adsorb in order to form H_2, HT, or T_2 [13].

2. A flux, R_{des} (at/m².s), going from the surface to the pore. For first order desorption [13],

$$R_{des} = \frac{RN_s zT}{A_v h}\theta\exp(-E_{des}/RT). \quad (3)$$

Where E_{des} is the activation energy of desorption (J/mol), θ is the surface coverage of the desorbing species, N_s is the number of sites on the surface of the grain (at/m²), A_v is Avogadro's number (mol⁻¹), and h is Planck's constant (J.s). For second order desorption [12],

$$R_{des} = \frac{RN_s zT}{A_v h}\theta^2\exp(-2E_{des}/RT). \quad (4)$$

3. A flux, R_{diss} (at/m².s), going from the surface back to the grain,

$$R_{diss} = \frac{RN_s zT}{A_v h}\theta\exp(-E_{diss}/RT). \quad (5)$$

Where, E_{diss} is the activation energy of dissolution (J/mol).

4. A flux, R_β (at/m².s), going to the surface from the bulk [11],

$$R_\beta = \frac{3\times10^{13}}{r_g S_{BET}\rho\sqrt{N_s}}C_b(1-\theta)\exp(-E_\beta/RT). \quad (6)$$

Where, C_b is the tritium concentration in the bulk just below the surface (at/m³), E_β is the

activation energy for adsorption from the bulk to the surface (J/mol), S_{BET} is the specific surface area (m^2/kg), r_g is the grain radius (m), and ρ is the theoretical density (kg/m^3). The four energies, E_{ads}, E_{des}, E_{diss}, and E_β are related through the activation energy of solution, E_s, and the heat of adsorption, Q [12]:

$$E_s = E_{ads} - E_{des} + E_{diss} - E_\beta , \quad (7)$$

$$Q = E_{des} - E_{ads} . \quad (8)$$

Eqs. (1), (3), (5), and (6) can be rewritten as:

$$R_{ads} = K_{ads} (1 - \theta), \quad (9)$$

$$R_{des} = K_{des}\, \theta, \quad (10)$$

$$R_{diss} = K_{diss}\, \theta, \quad (11)$$

$$R_\beta = K_\beta (1 - \theta)\, C_b, \quad (12)$$

$$K_{ads} = \frac{\sigma . z}{\sqrt{8\times10^{-3}\pi}} \sqrt{\frac{RT}{M}} C_p \exp(-E_{ads}/RT) , \quad (13)$$

$$K_{des} = \frac{RN_s zT}{A_v h} \exp(-E_{des}/RT) , \quad (14)$$

$$K_{diss} = \frac{RN_s zT}{A_v h} \exp(-E_{diss}/RT) , \quad (15)$$

$$K_\beta = \frac{3\times10^{13}}{r_g S_{BET} \rho \sqrt{N_s}} \exp(-E_\beta/RT) . \quad (16)$$

The equations that describe the surface fluxes, Eqs. (9)and (12), are used to calculate the tritium surface coverage, θ_T, and the tritium grain concentration, C_b. In the case of absence of protium in the purge gas, the total surface coverage (θ) in the above equations is equal to the tritium surface coverage (θ_T). When protium is added, the fraction of filled sites (θ) will be equal to ($\theta_T + \theta_H$). The tritium surface inventory, I_s (g), is related to the surface coverage by [13]

$$I_s = \frac{\theta_T N_s S_{BET} \rho V_{br} M(1-\varepsilon)}{A_v} , \quad (17)$$

$$I_g = \left(C_b + \frac{g r_g^2}{15D} \right) \frac{V_{br} M(1-\varepsilon)}{A_v} . \quad (18)$$

Where V_{br} is the breeder volume (m^3) and ε it's porosity. The grain inventory, I_g (g), can be obtained from C_b, D is the diffusion coefficient of tritium in the grains (m^2/s). In this case g is the rate of tritium generation per unit volume of the breeder ($at/m^3.s$). The total tritium inventory in the breeder is equal to

$$I_{tot} = I_s + I_g . \quad (19)$$

Case 1: First order adsorption/ desorption

For the case of steady state tritium generation and release, the net flux coming out of the pores is equal to the tritium generated inside the grains. Therefore,

$$R_{des,T} - R_{ads,T} = g. \quad (20)$$

Where, g is the effective rate of tritium generation per unit surface area ($at/m^2.s$).
If no H_2 is present in the purge gas the surface will be covered with only tritium. Therefore, the total surface coverage θ will be equal to the tritium coverage θ_T. Rewriting Eq. (20)

$$K_{des}\, \theta_T - K_{ads,T} (1 - \theta_T) = g \quad (21)$$

Note that K_{des} does not depend on whether the flux is that of tritium or hydrogen, whereas K_{ads} is isotope-dependent through both the molecular weight and the pore concentration of the adsorbed gas. Hence, the subscript (T) will denote the tritium while the subscript (H) will denote the protium.
Solving eq. (21) for the tritium surface coverage we get:

$$\theta_T = \frac{g + K_{ads,T}}{K_{des} + K_{ads.T}} . \quad (22)$$

Since the net flux leaving the grain must also be equal to the generated tritium, we can write:

$$R_\beta - R_{diss} = g, \quad (23)$$

$$K_\beta C_b(1-\theta_T) - K_{diss}\,\theta_T = g. \quad (24)$$

Substituting for θ_T with Eq. (22), we get

$$C_b = \frac{g(K_{des} + K_{ads,T} + K_{diss}) + K_{diss}K_{ads,T}}{K_\beta(K_{des} - g)}. \quad (25)$$

In the presence of H_2 in the purge gas, the equations become more complicated due to the fact that the surface sites will be covered with both protium and tritium, i.e.

$$\theta_{tot} = \theta_T + \theta_H. \quad (26)$$

Thus an additional equation is required to account for θ_H. This can be obtained from equating both the desorption and adsorption fluxes of protium at steady state (since no protium is generated in the breeder)

$$R_{des,H} = R_{ads,H}, \quad (27)$$

$$K_{des}\,\theta_H = K_{ads,H}\,(1-\theta_{tot}). \quad (28)$$

Again for tritium, solving Eq. (20) we get:

$$K_{des}\,\theta_T = K_{ads,T}\,(1-\theta_{tot}) = g. \quad (29)$$

Solving Eqs. (26), (28), and (29) we obtain two equations that describe the surface coverage of tritium and protium in terms of the different flux coefficients:

$$\theta_T = \frac{g(K_{des} + K_{ads,H}) + K_{des}K_{ads,T}}{K_{des}(K_{des} + K_{ads,T} + K_{ads,H})}, \quad (30)$$

$$\theta_H = \frac{K_{ads,H}(K_{des} - g)}{K_{des}(K_{des} + K_{ads,T} + K_{ads,H})}, \quad (31)$$

$$K_\beta C_b(1-\theta_{tot}) - K_{diss}\theta_T = g. \quad (32)$$

Equation (23) is used to obtain the tritium grain concentration

$$C_b = \frac{K_{ads,T}(g + K_{diss}\theta_T)}{K_\beta(K_{des}\theta_T - g)}. \quad (33)$$

Case 2: Second order adsorption/ desorption

For second order surface processes, the same basic equations are used. However, the term $(1-\theta)$ in the adsorption flux is squared together with the term θ in the desorption flux. Also in K_{des} and K_{ads}, the activation energies are doubled. Therefore, for steady state conditions with no H_2 in the purge gas, solving Equation 20 gives:

$$K_{des}\theta_T^2 - K_{ads,T}(1-\theta_T)^2 = g. \quad (34)$$

Solving for θ_T we get:

$$\theta_T = \frac{-K_{ads,T} + \sqrt{K_{ads,T}^2 + (g + K_{ads,T})(K_{des} - K_{ads,T})}}{K_{des} - K_{ads,T}}. \quad (35)$$

The tritium bulk concentration can be obtained from Eq. (23),

$$C_b = \frac{g + K_{dss}\theta_T}{K_\beta(Y1 - \theta_T)}. \quad (36)$$

For the addition of protium to the purge gas, there will be two different gases containing protium in the system, namely, H_2 and HT. By equating the different protium adsorbing and desorbing fluxes, we get:

$$K_{des}\theta_{tot}\theta_H = K_{ads,H}(1-\theta_{tot})^2. \quad (37)$$

The term $\theta_{tot}\theta_H$ is due to the addition of a term containing $\theta_H\theta_H$, of the desorbing H_2 flux and a term containing $\theta_T\theta_H$ of the desorbing HT flux [13].
Similarly, for tritium, considering that there are two tritium containing gases; T_2 and HT, we get:

$$K_{des}\theta_{tot}\theta_T - K_{ads,T}(1-\theta_{tot})^2 = g. \quad (38)$$

Solving Eqs. (37), (38), and (26), we get a relation between the total surface coverage and that of tritium:

$$\theta_{tot} = \frac{K_{tot} - \sqrt{K_{tot}^2 - (g + K_{tot})(K_{tot} - K_{des})}}{K_{tot} - K_{des}}, \quad (39)$$

$$K_{tot} = K_{ads,T} + K_{ads,H}, \quad (40)$$

$$\theta_T = \frac{g + K_{ads,T}(1 - \theta_{tot})^2}{K_{des}\theta_{tot}}. \quad (41)$$

The tritium concentration in the grain is then obtained from Eq. (32).

3. Examination of tritium transport phenomena

The tritium release behavior from Li_2O and $LiAlO_2$ was studied in a set of experiments named as TTTEx [6-10]. In these experiments, the samples were irradiated, and the amount of tritium released was measured at different temperatures and purge gas compositions. Although the experiments were made using Li_2O and $LiAlO_2$, only Li_2O data are used in the analysis because: (1) it is one of the major candidates for the reactor blanket [13], and, (2) experimental data are available for Li_2O properties such as diffusion, desorption, adsorption and solubility [14]. This data is not readily available for other ceramic breeders.

Some of the sample and purge gas characteristics are summarized in Table 1. Those values are used to examine the surface and grain inventories and their relation with the temperature and H_2 concentration in the purge gas, for both first and second order surface reactions. The values in Table 1 were used to calculate the flux coefficients K_{des}, K_{ads}, K_β and K_{diss}. The tritium concentration $C_{p,T}$ was calculated from [12]:

$$C_{p,T} = \frac{gV_{br}(1-\varepsilon)}{Q}. \quad (42)$$

Where, Q is the purge gas flow rate (m^3/s).

3.1 Effect of temperature

Figure 2 shows the change in surface, grain and total tritium inventories with temperature for first order reactions in the absence of H_2 in the purge gas. As expected, the inventory decreases with increasing temperature, since all of the processes are temperature-enhanced. I_{tot} decreases by 4 orders of magnitude between 350°C and 900°C. Although the total tritium inventory is almost equal to that in the grain, it is important to include surface processes when calculating the inventory. This is because the surface fluxes act as a barrier that slows down the tritium release, hence increasing the tritium inventory.

Table 1 Summary of the used TTTEx experimental data [6-10].

Sample mass (g)	0.79
Porosity	0.22
Specific surface area (m^2/kg)	0.09
Sample volume (m^3)	5.32×10^{-4}
Grain radius (μm)	1.9
Rate of tritium generation (at/m^3)	2.83×10^{12}
Helium pressure (atm)	1
Flow rate (m^3/s)	2×10^{-6}

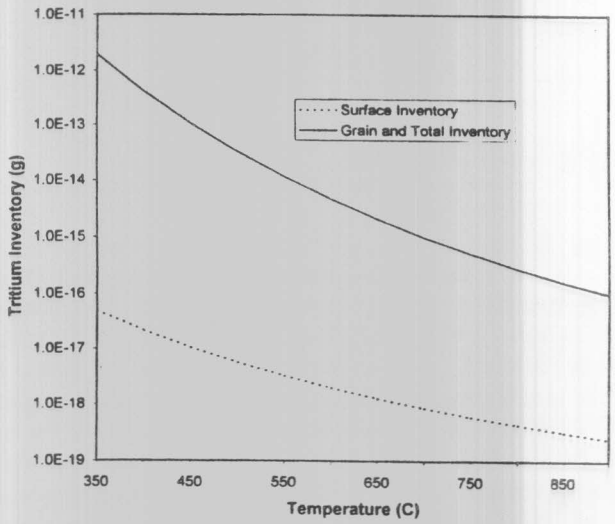

Fig. 2. Effect of temperature on tritium inventory for first order reactions in the absence of H_2 in the purge gas.

In Fig. 3 the change in inventory with temperature for second order adsorption/desorption processes in the absence of H_2 in the purge gas is shown. The

inventory is again found to decrease with increasing temperature. However, most of the inventory in this case is located on the surface, which is consistent with the findings of Nishikawa et al. [3] that in the absence of H_2 in the purge gas the surface inventory can be larger than that in the grain. This can be explained by noting that second order desorption is more difficult than first order desorption, because two atoms are required to combine and desorb together [11]. This makes it harder for tritium atoms to leave the surface, which causes an increase in the surface inventory.

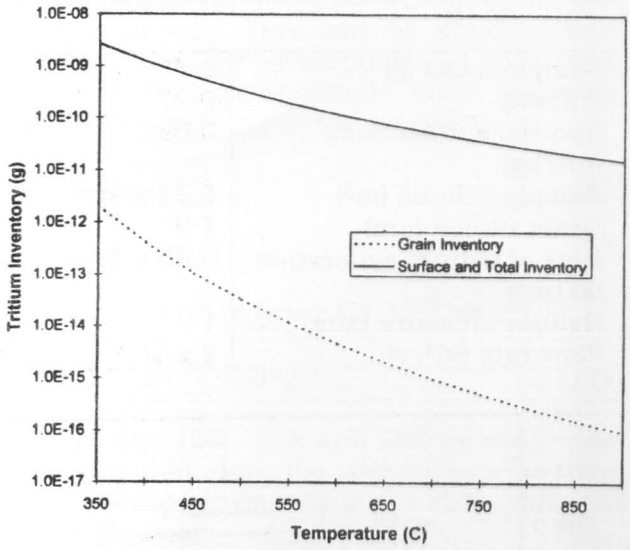

Fig. 3. Effect of temperature on tritium inventory for second order reactions in the absence of H_2 in the purge gas.

It can be seen from Figures 2 and 3 that the total inventory for the first order processes is much less that that in the second order case (about 2-3 orders of magnitude lower). For Li_2O samples, the tritium inventory in the TTTEx experiments was between 10^{-8}–10^{-10}g at 410°C [9]. Comparison between the experimental and analytical results suggests that the surface processes are indeed second order and not first order processes.

Figure 4 shows the change in surface, grain and total tritium inventories with temperature for first order reactions in the presence of 1% H_2 in the purge gas. The figure is almost identical to Fig. 2, suggesting a negligible influence of adding H_2 to the purge gas. This is in contrast to the experimental finding [6].

Figure 5 shows the effect of temperature on the tritium inventory for second order reactions in the presence of 1% H_2 in the purge gas. The surface inventory is less than in the case without protium (Figure 3). For example, at 600°C I_s decreased from 1.2 x10^9g to 6.3 x 10^{-14}g when 1% H_2 was added to the purge gas. This is due to the swamping effect of the H_2 that competes with the tritium on the surface [10]. The surface inventory decreases with temperature, whereas the grain inventory decreases with temperature until about 600°C then starts to increase slightly. In order to explain this behavior, Eq. (32) can be rewritten as,

$$C_b = \frac{g}{K_\beta(1-\theta_{tot})} + \frac{K_{diss}\theta_T}{K_\beta(1-\theta_{tot})}. \qquad (43)$$

The first term in the RHS of Eq. (43) decreases with temperature, whereas the second term increases with temperature. At high temperatures the second term starts to dominate, causing a net increase in the tritium grain concentration and hence inventory.

The total inventory decreases with temperature before 600°C, as both I_s and I_g decrease with increasing temperature. After 600°c, the combination of a decreasing I_s and an increasing I_g produce a total inventory that does not change with temperature.

3.2. *Effect of H_2 concentration*

Figure 6 shows the effect of increasing the H_2 concentration in the purge gas on the tritium inventory for first order reactions at 650°C. The figure shows that the addition of H_2 to the helium purge gas has no effect on I_s, I_g, or the total inventory.

In all cases, θ_T was very small ($\approx 4 \times 10^{-13}$) and stayed constant for all H_2 concentration. Again this is in contrast with the experiment findings that adding H_2 to the He sweep gas decreases the tritium inventory [16,17].

In Fig. 7, the effect of H_2 concentration on the tritium inventory for second order surface reactions at 650°C is shown. Adding H_2 to the

purge gas decreases the inventory. The grain, surface, and total inventories decreased until the H_2 concentration reached about 1%. After this concentration, an increase in the amount of H_2 did not change the total tritium inventory. This was reported by Terai et al. [18] who found that the tritium residence time decreases with increasing concentration of H_2 in helium sweep gas up to a limit concentration above which it becomes constant.

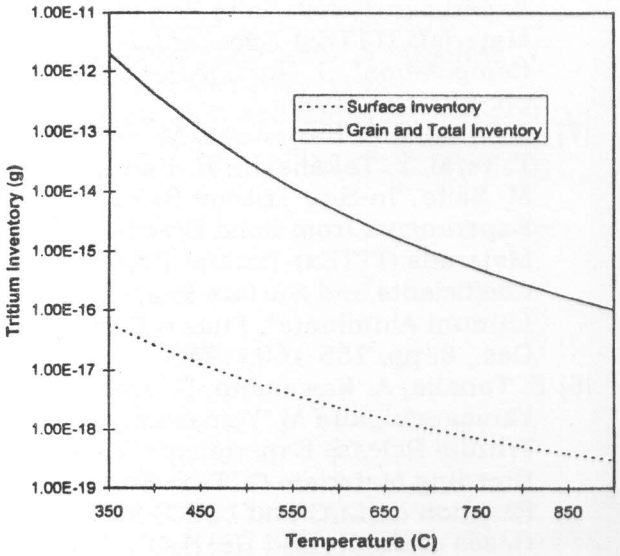

Fig. 4. Effect of temperature on tritium inventory for first order reactions in a sweep gas of He + 1%H_2.

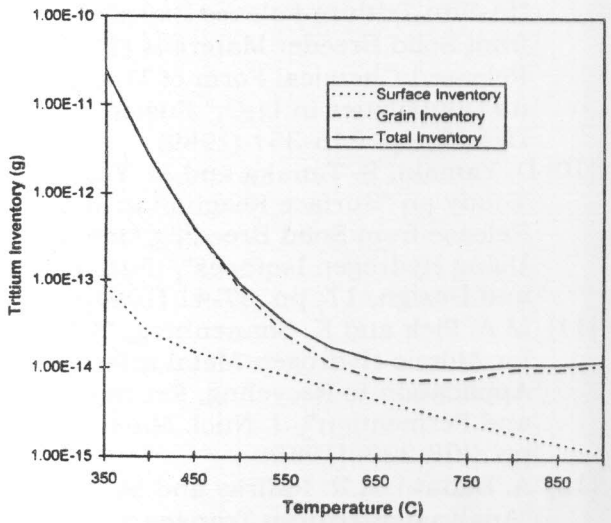

Fig. 5. Effect of temperature on tritium inventory for second order reactions in a sweep gas of He + 1%H_2 at 650°C.

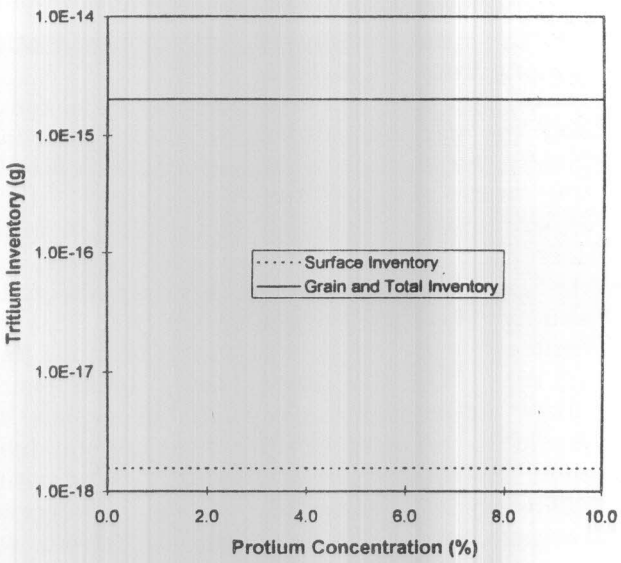

Fig. 6. Effect of H_2 concentration in the purge gas on the tritium inventory at 650°C for first order reactions.

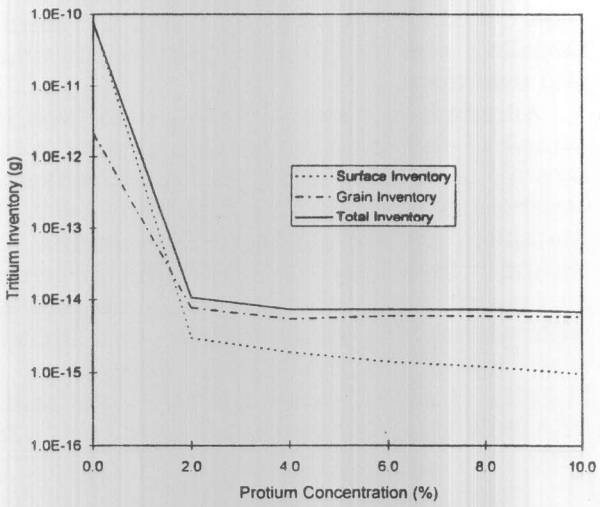

Fig. 7. Effect of H_2 concentration in the purge gas on the tritium inventory at 650°C for second order reactions.

4. Conclusion

Analyses of the tritium inventory in fusion ceramic breeders were made under steady state conditions, using first and second order adsorption/desorption processes on the surface. The resulting equations were used to calculate the grain and surface inventories for

different temperatures ranging from 350°C to 900°C, and different H_2 concentrations ranging from 0% to 10%.

Comparison between the analytical results and the experimental data shows that using first order surface reactions cannot reproduce the same tritium behavior found in the experiments. Although the tritium inventory decreases with increasing temperature, as in the experimental results, it is not affected by adding H_2 to the helium sweep gas. This is in contrast with the experimental findings [6, 8-10,16]. On the other hand, using second order adsorption/desorption processes was found to produce results that are consistent with the experimental results. The tritium inventory decreased with increasing temperature. The inventory decreased with increasing H_2 concentration up to a limit then remained constant for large values of H_2 concentration (>1%). This leads to the conclusion that in order to study the behavior of tritium inside the ceramic breeders, second order surface processes must be used in modeling and calculating the tritium release and inventory.

Although the analysis used data from Li_2O samples, the same conclusion applies to most ceramic breeders, since the same behavior is observed when other materials are used. For example, in the TTTEx experiments, the tritium inventory in the $LiAlO_2$ samples decreased with increasing temperature and with adding H_2 to the purge gas. The same was found in EXOTIC-6 experiment for Li_2ZrO_3, Li_4SiO_4, and $LiAlO_2$ [19] and in BEATRIX II experiment for Li_2O and Li_2ZrO_3 [20].

References

[1] A.R. Raffray, Z.R. Gorbis, and M.A. Abdou, "Rate Controlling Tritium Transport Mechanisms in Solid Breeders", Fusion Technol., 19, pp. 1525-1531 (1991).

[2] M.C. Billone, "The Influence of Surface Desorption on Tritium Recovery and Inventory in Fusion Solid Breeders", J. Nucl. Mater., 141-143, pp. 316-320 (1986).

[3] A.K. Fischer, "Processes for Desorption from $LiAlO_2$ Treated with H_2 as Studied by temperature programmed desorption,' Fusion Technol., 19, pp. 1012-1017 (1991).

[4] M. Nishikawa, A. Baba, and Y. Kawamura, J. Nucl. Mater., 246, pp. 1-8 (1997).

[5] J.P. Kopasz and C.E. Johnson, "Tritium Transport Modeling", DOE/ER-031316, Argonne National Laboratory, May (1989).

[6] S. Tanaka, T. Terai, H. Mohri, and Y. Takahashi, "In-Situ Tritium Release Experiments from Solid Breeding Materials (TTTEx)-Effect of Sweep Gas Composition", J. Nucl. Mater., 155-157, pp. 533-537 (1988).

[7] S. Tanaka, A. Kawamoto, M. Yamawaki, T. Terai, Y. Takahashi, H. Kawamura, and M. Saito, 'In-Situ Tritium Release Experiments from Solid Breeding Materials (TTTEx)-Tritium Diffusion Coefficients and Surface Reaction on Lithium Aluminate", Fusion Eng. and Des., 8, pp. 155-160 (1989).

[8] S. Tanaka, A. Kawamoto, D. Yamaki, K. Yamaguchi, and M. Yamawaki, "In-Situ Tritium Release Experiments from Solid Breeding Materials (TTTEx)-Surface Reaction on Li_2O and $LiAlO_2$ for Sweep Gases of $He+H_2$ and $He+H_2O$", J. Nucl. Mater., 179-181, pp. 867-870 (1991).

[9] T. Terai, Y. Takahashi, and S. Tanaka, "In-Situ Tritium Release Experiments from Solid Breeder Materials (TTTEx)–Released Chemical Form of Tritium and its Diffusivities in Li_2O," Fusion Eng. and Des., 7, pp. 345-351 (1989).

[10] D. Yamaki, S. Tanaka and M. Yamawaki, 'Study on "Surface Reaction in Tritium Release from Solid Breeding Materials by Using Hydrogen Isotopes", Fusion Eng. and Design, 17, pp. 37-41 (1991).

[11] M.A. Pick and K. Sonnenberg, "A Model for Atomic Hydrogen-Metal Interactions – Application to Recycling, Recombination and Permeation", J. Nucl. Mater., 131, pp. 208-220 (1985).

[12] A. Badawi, A.R. Raffray and M. A. Abdou, "Analysis of Tritium Transport Mechanisms at the Surface of Lithium Ceramics", Fusion Technol., 21, pp. 1939-1943 (1992).

[13] G. Federici, A.R. Raffray and M.A. Abdou, "A Comprehensive Model for Tritium Transport in Lithium-Base Ceramics- Part I: Theory and Description of Model Capabilities", J. Nucl. Mater., 173, pp. 185-213 (1990).

[14] M.C. Billone, "Thermal and Tritium Transport in Li_2O and Li_2ZrO_3", J. Nucl. Mater., 233-237, pp. 1462-1466 (1996).

[15] M.C. Billone, H. Attaya and J.P. Kopasz, "Modeling of Tritium Behavior in Li_2O", Argonne National Laboratory, ANL/FP/TM-260, August (1992).

[16] R.G. Clemmer et al., "The TRIO Experiment", ANL-84-55, Argonne National Laboratory (1984).

[17] H. Werle, J.J. Abassin et al., " The LISA1 Experiment: In-Situ Tritium Release Investigations", J. Nucl. Mater., 141-143, pp. 321-326 (1986).

[18] T. Terai, Y. Takahashi, S. Tanaka, and M. Yamawaki, "Modeling of Tritium Recovery from CTR Solid Breeder,' Fusion Eng. and Des., 8, pp. 349-354 (1989).

[19] H. Kwast, R. Conrad, R. May, S. Casadio, N. Roux, and H. Werle, "The Behavior of Ceramic Breeder Materials with Respect to Tritium Release and Pellet/Pebble Mechanical Integrity", J. Nucl. Mater., 212-215, pp. 1010-1014 (1994).

[20] R.A. Verrall, O.D. Slagle, G.W. Hollenberg, T. Kurasawa, and J.D. Sullivan, "Irradiation of Lithium Zirconate Pebble-Bed" J. Nucl. Mater., 212-215, pp. 902-907 (1994).

Received November 8. 1999
Accepted December 25. 1999